ACS APPLIED MATERIALS & INTERFACES

www.acsami.org

Research Article

Crosslinking Methodology for Imidazole-Grafted Silicone Elastomers Allowing for Dielectric Elastomers Operated at Low Electrical Fields with High Strains

Zhaoqing Kang, Liyun Yu, Yi Nie,* and Anne Ladegaard Skov*

Cite This: *ACS Appl. Mater. Interfaces* 2022, 14, 51384–51393

Read Online

ACCESS | Metrics & More | Article Recommendations | Supporting Information

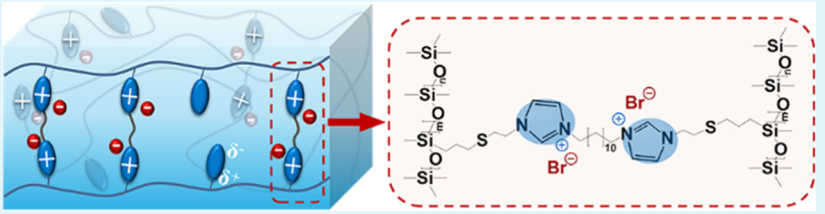

ABSTRACT: For improved actuation at low voltages of dielectric elastomers, a high dielectric permittivity has been targeted for several years but most successful methods then either increase the stiffness of the elastomer and/or introduce notable losses of both mechanical and dielectric nature. For polydimethylsiloxane (PDMS)-based elastomers, most high-permittivity moieties inhibit the sensitive platinum catalyst used in the addition curing scheme. In contrast to the classical addition curing pathway to prepare PDMS elastomers, here, an alternative strategy is reported to prepare PDMS elastomers via the crosslinking reaction between multifunctional imidazole-grafted PDMS with difunctional bis(1-ethylene-imidazole-3-ium) bromide ionic liquid (bis-IL). The prepared IL-elastomer entails uniformly dispersed IL and presents stable mechanical and dielectric properties due to the covalent nature of the crosslinking as opposed to previously reported physical mixing in of ILs. The relative permittivity was improved up to 200% by including the bis-IL in the elastomer, and Young's modulus was around 0.04 MPa. As a result of the excellent combination of properties, the dielectric actuator developed exhibits an area strain of 20% at 15 V/μm. The novel strategy to prepare PDMS elastomers provides a new paradigm for achieving high-performance dielectric elastomer actuators by a simple methodology.

KEYWORDS: *dielectric elastomer, actuator, ionic liquid, stability, chemical modification, homogeneity*

1. INTRODUCTION

Soft actuators based on electro-active polymers and elastomers have drawn great research and commercial interest over the last 30 years due to their inherent promise of overcoming the limitations of classical rigid actuators.[1] Dielectric elastomer actuators (DEAs) are one such type of soft actuators with advantages over classical actuators due to their softness and their potential for large actuation strains and high energy densities.[2−4] Furthermore, DEAs can reversibly alter their size or shape in response to an external applied electric field;[5,6] therefore, they have shown promising applicability in many fields, such as soft robotics, sensors, energy harvesters, and artificial muscles.[7,8] Among the possible elastomer candidates for DEAs, polydimethylsiloxane (PDMS) is one of the most promising ones due to its relatively low elastic modulus, fast response, and chemical and physical inertness.[9−11] However, the required high driving voltages to actuate (typically 500 V–10 kV)[12] have limited the commercial exploitation of DEAs as artificial muscles and soft robotics.

According to Pelrine et al.,[13] the thickness strain (s_z) of DEAs, based on the assumptions of small deformations, constant elastic modulus, and free boundary conditions, can be described by

$$s_z = -\frac{\varepsilon_0 \varepsilon_r}{Y}\left(\frac{U}{d}\right)^2 \quad (1)$$

where ε_0 is the vacuum permittivity (8.85×10^{-12} F m^{-1}), ε_r is the relative permittivity, Y is Young's modulus (also commonly referred to as the elastic modulus), U is the applied voltage, and d is the initial elastomer thickness. Therefore, the achievable actuation strain at a given voltage can be improved by either single parameter variation or simultaneous optimization of the three parameters. The optimal way according to the actuation equation is to simultaneously increase ε_r and reduce Y and d. However, this may not be the

Received: September 7, 2022
Accepted: October 24, 2022
Published: November 7, 2022

ideal approach seen from the perspective of improved reliability and lifetime. DEAs operating at low voltages (~250 V) have been developed by reducing the thickness of the dielectric elastomer below 20 μm[14,15] since the actuation strain at a given voltage scales inversely with the squared initial film thickness. However, reliable and reproducible fabrication of the dielectric films below 20 μm is challenging and costly with existing methodologies. Another way to prepare DEAs operating at low voltages is using soft elastomers, which can be prepared by, for example, reducing the crosslinking density[16] or by crosslinking of bottle brush PDMS.[17,18] However, most DEAs suffer from a low level of tangible forces of the actuator due to the combination of both low Y and low ε_r. Thus, focus in this work is on achieving large strain and low voltages by simultaneously increasing ε_r and lowering Y with inclusion of ionic liquids (ILs) grafted to the polymer chains in order to avoid the ILs to migrate under the high electrical field.

Also, the required voltage of the DEAs can be reduced by increasing the relative permittivity of the elastomers. The original method for this is to incorporate high-permittivity fillers, such as titanium dioxide,[19] zinc oxide,[20] and conductive carbons.[21] However, the increased ε_r is accompanied by a significant increase in the elastic modulus as well, so the overall improvement in actuation is usually limited.[12] Many synthesis approaches to enhancing the dielectric permittivity by chemical modification of the elastomers have been developed with polar groups,[22,23] such as porphyrin,[24] nitrobenzene,[25] phenyl,[26] and nitroaniline.[27] However, classical PDMS elastomers are mainly prepared by the addition curing pathway by means of a platinum catalyst, and the aforementioned strong dipoles will inhibit curing to greater or lesser extent.[9] Although significant actuation was achieved through elastomers with a combination of increased ε_r and resulting softness from the unreacted moieties as a result of the partial inhibition, the mechanical properties of the elastomers were not reliable over time under load and/or electrical voltage due to the viscous dissipative nature of the resulting elastomers.[25,27] Therefore, it is necessary to develop reproducible and insensitive crosslinking reaction methodologies to achieve well-crosslinked elastomers and thus reliable DEAs.

ILs, which are regarded as environmentally friendly chemicals, have high thermal and chemical stabilities and have been shown to result in a remarkable improvement of ε_r of PDMS elastomers due to the space charge polarization of the ions under applied electric field.[28,29] Furthermore, like other liquid fillers, ILs can also be regarded as soft fillers that decrease the Y of the resulting elastomers due to a combination of inhibition and plasticization effects.[30,31] Mathews et al.[32] investigated a PDMS elastomer with 20% 1-ethyl-3-methyl-imidazolium bis(trifluoromethylsulfonyl) imide and presented a 2-fold increase in ε_r and 100-fold decrease in Y, achieving ~6% area strain at 4 V/μm. Shi et al.[33] reported a PDMS elastomer with ~22% propyl-methyl-imidazolium bis-(fluorosulfonyl) imide, which showed a sevenfold increase in ε_r and threefold decrease in Y. However, when ILs are incorporated in the composites without strong chemical bonds to the network, they will inherently aggregate in the PDMS matrix over time due to the immiscibility of PDMS and ILs.[34] In addition, a strongly inhibiting effect of the IL on the platinum catalyst used for curing of the PDMS elastomer was observed in a previous study,[35] indicating that the mechanical properties of the elastomer may not be stable as a lot of reactive species are present and may react further or migrate.

To overcome the above challenges, one potential way is chemically grafting a PDMS polymer with IL and then crosslinking the polymer into an elastomer via a nucleophilic substitution reaction.[36] Previously, we prepared a dielectric elastomer by using this method; however, the synthesis approach, various parameters for this approach, and the actuation performance of the resultant elastomers have not been optimized.[37]

Here, we report a strategy for covalently anchoring a bis(1-ethylene-imidazole-3-ium) bromide IL (bis-IL) to a commercially available mercapto-propyl functional PDMS polymer to yield a PDMS grafted with multiple ILs per polymer chain. Finally, crosslinking by means of the IL entities is performed to yield an elastomer. This approach limits phase separation during curing and over time. The prepared IL-elastomers possess uniform dispersion of IL and present stable mechanical and dielectric properties due to the covalent integration of IL into the network structure as opposed to the previously explored physical incorporation of IL into silicone elastomers. Furthermore, the IL contributes to an improved relative permittivity of the IL-elastomers. With the combination of high ε_r and low Y, the IL-elastomers are shown to have outstanding actuation performance and pose a promising potential for use as dielectric elastomers for a plethora of soft devices.

2. EXPERIMENTAL SECTION

2.1. Materials. The mercaptopropyl silicone SMS-042 [4–6%(mercaptopropyl)methylsiloxane]dimethylsiloxane copolymer (M_n = 6000–8000 g mol^{-1}, four–five mercaptopropyl groups per polymer) was purchased from Gelest Inc. 1-Vinylimidazole (Vim), azobisisobutyronitrile (AIBN), chloroform, and 1,12-dibromododecane (DBD) were obtained from Sigma-Aldrich Co., Ltd. All chemicals were used as received without further purification.

2.2. Synthesis of Imidazole-Grafted Silicone (Im-g Silicone). The Im-g silicone was synthesized through the thiol–ene addition of the mercaptopropyl silicone and Vim. The mercaptopropyl silicone (21.0 g, 3.0 mmol), Vim (1.2 g, 14.0 mmol), and AIBN (22.2 mg, 0.1 wt % of the reactants) were added to a 100 mL single-neck round-bottom flask and dissolved in 50 mL of chloroform. The molar ratio between sulfhydryl groups on the mercaptopropyl silicone and vinylimidazole groups was 1:1. The reaction mixture was deoxygenated by bubbling nitrogen for 10 min; then, the flask was sealed with a rubber stopper. The reaction was then run at 60 °C for 15 h, after which the reaction was stopped by cooling the flask to ambient temperature. The purification process was performed as follows: the initial product was obtained by removing chloroform in a rotary evaporator, and then the product was rinsed three times with deionized water to extract any unreacted Vim. The final product (Im-g silicone) was obtained after drying in a vacuum oven for 24 h at room temperature. Im-g silicone: ^{1}H NMR ($CDCl_3$): δ 7.51 (s, 1H), 7.06 (s, 1H), 6.94 (s, 1H), 4.11 (t, J = 7.0 Hz, 2H), 2.82 (t, J = 7.0 Hz, 2H), 2.44 (t, J = 7.4 Hz, 2H), 1.75–1.43 (m, 2H), 0.58 (t, J = 8.4 Hz, 2H), and 0.07 (s, 111H).

2.3. Preparation of IL-Elastomer. IL-elastomers were prepared by a nucleophilic substitution reaction of the Im-g silicone with DBD. Im-g silicone (2.0 g, 0.3 mmol) and given amounts of DBD were mixed 5 min at 3500 rpm using a dual asymmetric centrifuge (FlackTek Inc. DAC 150.1 FVZ-K SpeedMixer). Thereafter, the uniform mixture was poured into a polytetrafluoroethylene mold with dimensions of 5 × 5 × 2.5 cm (width × length × thickness). The resulting film was cured at 80 °C for 3 h in an oven. As presented in Table 1, IL-elastomers 1–5 with different amounts of DBD were prepared by using molar ratios (r) of bromine over imidazole groups equal to 0.4, 0.5, 0.6, 0.7, and 0.8, respectively. As shown in Figure S1, the eluted products of all IL-elastomers in the swelling experiment did not present the chemical shift at 3.4 ppm (peak 3) which represents pristine DBD, indicating that DBD has reacted fully with Im-g

https://doi.org/10.1021/acsami.2c16086
ACS Appl. Mater. Interfaces 2022, 14, 51384–51393

Table 1. Amounts of Reagents Used for the IL-Elastomer Preparation and the Weight Fractions of Bis-IL in the Elastomers

sample	m(Im-g silicone) (g)	m(DBD) (g)	r	$w_{bis\text{-}IL}$ (%)
IL-elastomer 1	2	0.08	0.4	6.0
IL-elastomer 2	2	0.10	0.5	7.5
IL-elastomer 3	2	0.12	0.6	8.9
IL-elastomer 4	2	0.14	0.7	10.3
IL-elastomer 5	2	0.16	0.8	11.7

silicone. Therefore, the weight fractions ($w_{bis\text{-}IL}$) of bis(1-ethylene-imidazole-3-ium) bromide IL (bis-IL) in the elastomers are calculated based on the full conversion of DBD.

2.4. Characterization. *2.4.1. Fourier Transform Infrared Spectroscopy.* Fourier transform infrared (FT-IR) spectra in the wavenumber range of 650−4000 cm^{-1} were acquired from a Nicolet-380 FT-IR instrument fitted with a diamond crystal attenuated total reflection accessory. All spectra were baseline corrected.

2.4.2. Proton Nuclear Magnetic Resonance. Proton nuclear magnetic resonance (^{1}H NMR) spectra were acquired from a 7 T Spectrospin-Bruker 300 MHz spectrometer by use of dilute solutions (100 mg mL^{-1}) in deuterated chloroform.

2.4.3. Tensile Strength, Strain at Break, and Young's Modulus. Tensile stress−strain diagrams were obtained using a material tester (Instron 3340 materials testing system, INSTRON, US). Measurements were conducted at room temperature. The films were cut in the shape of 20 mm length and 3 mm width before the samples were placed between the two clamps separated by a distance of 10 mm. The test specimen was elongated uniaxially with a speed of 10 mm min^{-1}. Y was determined from the tangent of the stress−strain curves at 10% strain. Three measurements were conducted for each sample, and the determined values of Y were averaged.

2.4.4. Linear Viscoelastic Properties. Linear viscoelastic properties of the samples were measured at room temperature (20 °C) using an ARES-G2 rheometer (TA Instruments) in the controlled strain mode with 0.5% strain and with frequency sweeps from 10^2 to 10^{-2} Hz. The used geometry was 25 mm parallel plate. According to the kinetic theory of rubber,[38] the crosslinking density (ν) of the IL-elastomers is determined as

$$\nu = \frac{G'}{RT} \tag{2}$$

where G' is the shear modulus, R is the gas constant (8.314 J K^{-1} mol^{-1}), and T is the absolute temperature. The molecular weight between crosslinks (M_c) is determined as

$$M_c = \frac{RT\rho}{G'} \tag{3}$$

where ρ is the density of PDMS (0.97 g cm^{-3}).

2.4.5. Thermogravimetric Analysis. Thermogravimetric analysis (TGA) was performed on a Mettler Toledo TGA2 Instrument under nitrogen with a heating rate of 10 °C min^{-1} in the temperature interval from 30 to 800 °C.

2.4.6. Swelling Experiments. Gel fractions were determined via swelling experiments according to our previously reported procedure,[26] where elastomer films of dimension 10.0 mm length × 10.0 mm width × 0.5 mm thickness were immersed in chloroform for 72 h at room temperature. The solvent was being replaced daily. After 3 days of swelling, the chloroform was decanted, and the films were washed with fresh chloroform several times. Subsequently, the films were dried for 2 days in an ambient atmosphere. The gel fractions were determined from

$$W_{gel} = \frac{m_1}{m_0} \times 100\% \tag{4}$$

where m_1 is the weight after extraction and drying and m_0 is the initial weight of the sample. In addition, the eluted products were investigated by ^{1}H NMR analysis to determine the content of synthesized bis-IL (Figure S1). The weight fraction ($w'_{bis\text{-}IL}$) of bis-IL in the eluted product is given by

$$w'_{bis-IL} = \frac{f_1 r_1 M_{bis-IL}}{f_2 M_{Img-silicone} + f_1 r_1 M_{bis-IL}} \times 100\% \tag{5}$$

where f_1 and f_2 are the functionality of Im-g silicone (five imidazole groups per polymer) and DBD (two bromine groups per molecule), respectively, r_1 is the mole ratio of the imidazole cation and imidazole group in the eluted product, which equals to the ratio of areas of peak 2 and peak 1 in Figure S1, and $M_{bis\text{-}IL}$ and $M_{Im\text{-}g\ silicone}$ are the molecular weight of bis-IL and imidazole-grafted silicone, respectively. The weight fraction of bis-IL ($w''_{bis\text{-}IL}$) as the crosslinker in IL-elastomers is described as

$$w''_{bis-IL} = \frac{m_0 w_{bis-IL} - (m_0 - m_1) w'_{bis-IL}}{m_0} \times 100\% \tag{6}$$

The content of bis-IL (c_{cro}) being active as a crosslinker is described as

$$c_{cro} = \frac{w''_{bis-IL}}{w_{bis-IL}} \times 100\% \tag{7}$$

The calculated $w'_{bis\text{-}IL}$, $w''_{bis\text{-}IL}$, and c_{cro} of the IL-elastomers are shown in Table S1.

2.4.7. Field-Emission Scanning Electron Microscopes. Field-emission scanning electron microscopy (FE-SEM) (SU8020, Hitachi) was used for the morphology investigation. Energy-dispersive X-ray spectroscopy (EDS) was used to record the element distribution profile on the sample surfaces. All samples were sputter coated with a 2 nm thick layer of platinum prior to testing.

2.4.8. Dielectric Relaxation Spectroscopy. The dielectric relaxation spectra of the samples were acquired using a Novocontrol Alpha-A high-performance frequency analyzer (Novocontrol Technologies GmbH & Co, Germany). The instrument was operated at 1 V mm^{-1} at room temperature and in the frequency range of 10^{-1} to 10^6 Hz.

2.4.9. Figure of Merit (F_{om}) Determination. The evaluation of performance of DEAs under constant voltage is commonly expressed by a figure of merit that combines the properties of elastomers to a single parameter. According to Sommer-Larsen and Larsen,[39] the figure of merit (F_{om}) for a given dielectric elastomer used as an actuator is described as

$$F_{om} = \frac{3\varepsilon_r \varepsilon_0 E_{BD}^2}{Y} \tag{8}$$

For easier comparison of the optimized properties of the IL-elastomers compared to those of a reference elastomer, a normalized figure of merit (F^*_{om}) for actuators was used in this work. The equation is given by

$$F^*_{om} = \frac{\varepsilon_r E_{BD}^2}{Y} \Big/ \frac{\varepsilon_{r,0} E_{BD,0}^2}{Y_0} \tag{9}$$

where $\varepsilon_{r,0}$, Y_0, and $E_{BD,0}$ represent the ε_r, Y, and electric breakdown strength of the reference elastomer, respectively. The chosen reference elastomer in this work is a pure PDMS elastomer ($\varepsilon_{r,0}$ = 2.5, Y_0 = 0.8 MPa, and $E_{BD,0}$ = 40 V/μm) prepared from the hydrosilylation reaction in previous work.[40,41]

2.4.10. Actuation Tests. The IL-elastomers were mounted on a rigid ring mold with an inner diameter of 50 mm. A biaxial prestrain of 5% was used. Circular carbon grease electrodes with approximately 100 μm thickness and with a diameter of 30 mm were cast on both sides of the elastomer films. The resulting electrodes were connected to a Stanford Research Systems model PS37 high-voltage source. The tests were performed by voltage increments of 500 V from 0 V to the voltage until the dielectric breakdown was recorded. The diameter of the circular carbon grease electrode was tracked using a digital video

https://doi.org/10.1021/acsami.2c16086
ACS Appl. Mater. Interfaces 2022, 14, 51384−51393

Scheme 1. (a) Synthesis of the Im-g Silicone Via Thiol−Ene Addition of Mercaptopropyl Silicone and Vim in the Presence of AIBN and (b) Preparation of IL-Elastomers by Nucleophilic Substitution of Im-g Silicone with DBD

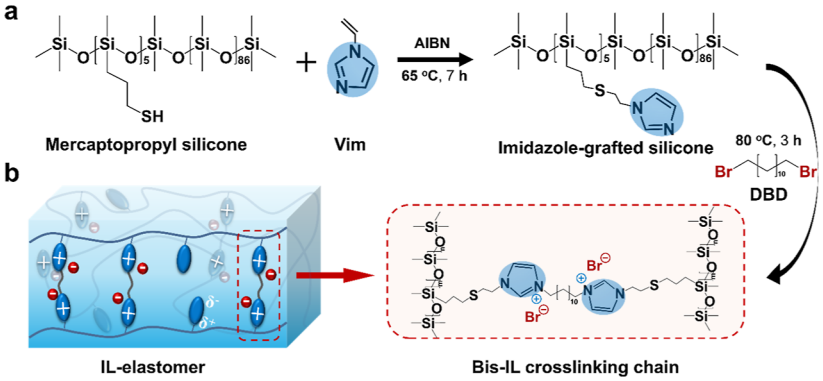

camera (LUMIX DMC-G80), and the resulting images were analyzed using the video analysis and modeling tool Tracker 6.0.1, which is a project of open-source physics hosted by comPADRE. The lateral strain (s_x), which is the relative change in the diameter of the circular actuator, is determined as

$$s_x = \frac{D_a - D_r}{D_r} \tag{10}$$

where D_a is the diameter of the circular electrode in the actuated state, and D_r is the diameter of the circular electrode before actuation. The area strain (s_A) is determined as

$$s_A = (s_x + 1)^2 - 1 \tag{11}$$

Assuming that the silicone elastomers are incompressible,[42] the thickness (d_r) of the elastomer film under prestrain is determined as

$$d_r = \frac{d_0}{(s_p + 1)^2} \tag{12}$$

where d_0 is the initial thickness of the elastomer film before prestrain and s_p is the biaxial prestrain of the elastomer film. The thickness (d_a) of the elastomer film in the actuated state is determined as

$$d_a = \frac{d_r}{(s_x + 1)^2} \tag{13}$$

The electric field can be calculated from

$$E = \frac{U}{d_a} = \frac{U}{d_0}(s_p + 1)^2(s_x + 1)^2 \tag{14}$$

where U is the applied voltage.

3. RESULTS AND DISCUSSION

The synthesis of the IL-elastomers is shown in Scheme 1. First, the multifunctional Im-g silicone was synthesized from a commercially available polymer by the thiol−ene addition of mercaptopropyl silicone and Vim in the presence of the AIBN initiator. Then, the IL-elastomers were prepared from Im-g silicone with difunctional bis-IL as the crosslinker. This new curing route avoids the inhibiting effect of IL on the classical platinum-catalyzed silylation curing of the PDMS elastomer.

3.1. Chemical Characterization. The extent of the thiol−ene addition between Vim and sulfhydryl groups on the mercaptopropyl silicone was investigated by ^{1}H NMR analysis. Peak 6 in Figure 1a represents the chemical shifts of the protons on the sulfur, and it vanishes after the thiol−ene addition with Vim (Figure 1b), indicating a complete conversion of sulfhydryl groups and thus a successful reaction. As presented in Figure 1b, peaks 9−11 in the spectrum

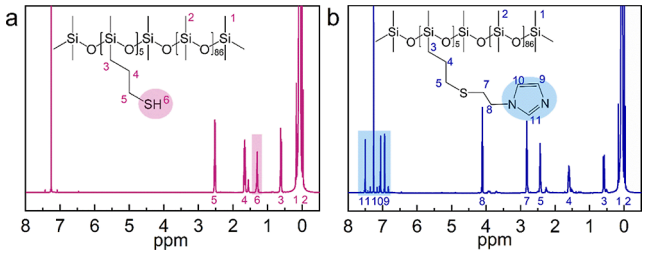

Figure 1. (a) ^{1}H NMR spectrum of mercaptopropyl silicone and (b) ^{1}H NMR spectrum of Im-g silicone.

attribute to the chemical shifts of protons on the imidazole ring, confirming that the Vim is grafted to the mercaptopropyl silicone. Furthermore, the integration of the peaks in Figure 1b provides clear evidence for the synthesis of Im-g silicone.

The IL-elastomers are cured based on a nucleophilic substitution reaction of Im-g silicone with DBD. FT-IR spectra were analyzed to verify the successful curing of the Im-g silicone. As shown in Figure 2a, the characteristic peaks

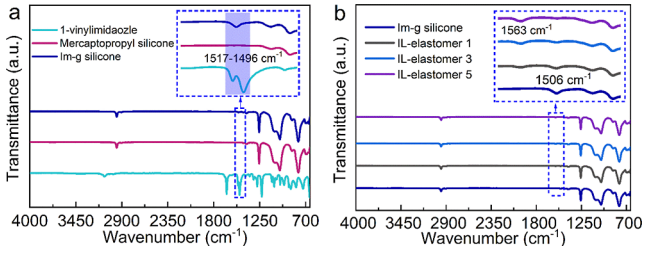

Figure 2. (a) FT-IR spectra of Vim, mercaptopropyl silicone, and Im-g silicone and (b) FT-IR spectra of Im-g silicone, IL-elastomer 1, IL-elastomer 3, and IL-elastomer 5.

between 1517 and 1496 cm^{-1} represent the imidazole ring. All elastomers in Figure 2b exhibit the characteristic peaks of the imidazole ring at 1563 cm^{-1}, while the unreacted Im-g silicone presents shifted characteristic peaks at ∼1506 cm^{-1}. This shifted signal confirms the successful conversion of the initial imidazole in Im-g silicone into imidazole cations in the IL-elastomers.[43,44] Furthermore, with the increase in the content of DBD from 3.8 to 7.4 wt % (IL-elastomer 1 to 5), the IL-elastomer presents an increased peak intensity at 1563 cm^{-1} and decreased peak intensity at ∼1506 cm^{-1}. This indicates that bis-IL content increased by increased DBD content in the Im-g silicone, as expected.

https://doi.org/10.1021/acsami.2c16086
ACS Appl. Mater. Interfaces 2022, 14, 51384−51393

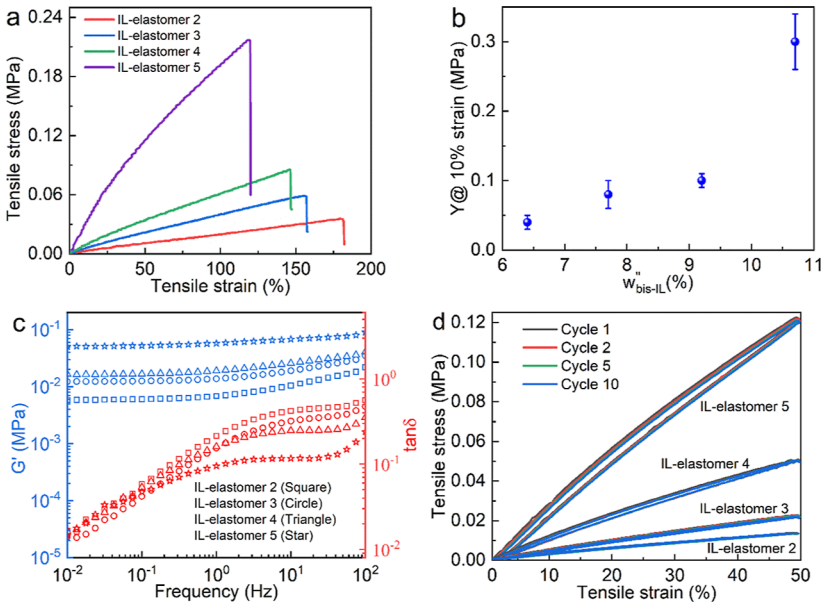

Figure 3. (a) Tensile stress−strain curves of IL-elastomers 2−5; (b) Young's modulus (Y) of IL-elastomers 2−5; (c) shear modulus (G') and relative viscous loss (tan δ) of IL-elastomers 2−5 measured at 0.5% strain; and (d) cyclic stress−strain curves up to 50% strain for IL-elastomers 2−5.

3.2. Gel Fraction. To understand better the network structures of the IL-elastomers, swelling experiments were conducted to quantify the content of covalently bonded (gel fraction) and nonbonded (sol fraction) species. As illustrated in Table S1, with an increased content of DBD from 3.8 to 7.4 wt %, the gel fractions increase from 50.3 to 87.1% (IL-elastomer 1−5). The gel fractions are not as high as that of the PDMS elastomers in our previous work,[35,45] but the crosslinking methodologies are also significantly different. However, mechanical and dielectric stabilities of the IL-elastomers were investigated further to ensure that the presence of nonbonded fractions does not impact the overall stability. The results are discussed in the Mechanical Properties and Dielectric Properties sections.

To further understand the resulting network structure of the resulting elastomers, the crosslinking density is investigated. The crosslinking density (ν) of the IL-elastomers is determined by the content of bis-IL that functions as the crosslinker. The weight fraction of bis-IL as the crosslinker ($w''_{\text{bis-IL}}$) in IL-elastomers is calculated according to eq 6. As illustrated in Tables S1 and S2, ν increases from 2.4 to 20.8 mol m^{-3} with $w''_{\text{bis-IL}}$ increasing from 6.4 to 10.7 wt %. In addition, the crosslinking efficiency (c_{cro}) of bis-IL can be estimated and it increases from 75 to 92% with the $w''_{\text{bis-IL}}$ increased from 4.5 to 10.7 wt %. The high crosslinking efficiency of bis-IL for the IL-elastomer proves a good crosslinking methodology. Pictures of the IL-elastomers with various bis-IL contents are shown in Figure S2. IL-elastomer 1 has too poor mechanical properties due to the low gel fraction (50.3%) and $w''_{\text{bis-IL}}$ (4.5%) and is thus not part of subsequent testing and evaluation.

3.3. Morphology. FE-SEM images of IL-elastomers 2−5 are shown in Figure S3a−d. All IL-elastomers display clear uniform morphologies with evenly arranged wrinkles. The wrinkles which also have been shown to prevail in other PDMS elastomers[26,45] may be formed due to a slight shrinking of the PDMS elastomer during curing. Figure S3e−h shows EDS images of IL-elastomer 3. The uniform dispersion of N and Br elements, which represent imidazole cations and bromine anions of the bis-IL, respectively, confirms that the bis-IL is uniformly distributed and thus indirectly confirms that the grafting is successful since phase separation would have been expected elsewise.

3.4. Thermal Stability. TGA was conducted to explore the temperature range in which the IL-elastomers are relevant to be used. As shown in Figure S4, all IL-elastomers present a two-stage thermal decomposition. The first stage, with a derivative thermogravimetric peak temperature of 318 °C, is related to the decomposition of IL. During the second stage, thermal decomposition of PDMS proceeds in the temperature range of 400−700 °C.[39,40] Taking into account that all IL-elastomers are thermally stable up to 270 °C where the initial onset of degradation is recorded, they can find potential application in high-temperature environments like other classical silicone elastomers.

3.5. Mechanical Properties. Tensile testing was performed to evaluate the linear properties of the elastomers as well as the ultimate properties. Data for Young's modulus, tensile strength, and strain at break of the IL-elastomers was acquired, and as shown in Figure 3a and Table S3, the stiffness of the IL-elastomer increases with increasing $w''_{\text{bis-IL}}$ from 6.4 wt % (IL-elastomer 2) to 10.7 wt % (IL-elastomer 5). The strains at break of the elastomers decrease from 182 to 121% in line with the increased stiffness. This can be attributed to the fact that the crosslinking density of the PDMS network increases and the chain mobility of the PDMS molecules between the junctions decreases with increasing crosslinking.[38] In addition, the ultimate tensile strength of the elastomers increases with increasing bis-IL content due to the increased crosslinking density.[46] Although all the IL-elastomers have low strains at break compared with commercial PDMS elastomers (~300%), they are still sufficiently flexible to be applied as DEAs since actuation strains usually are below 50%.[12]

As shown in Figure 3b, all elastomers show rather low Y (such as 0.04 MPa for IL-elastomer 2) compared to commercial PDMS elastomers (~1 MPa).[9] A reduced Y

https://doi.org/10.1021/acsami.2c16086
ACS Appl. Mater. Interfaces 2022, 14, 51384−51393

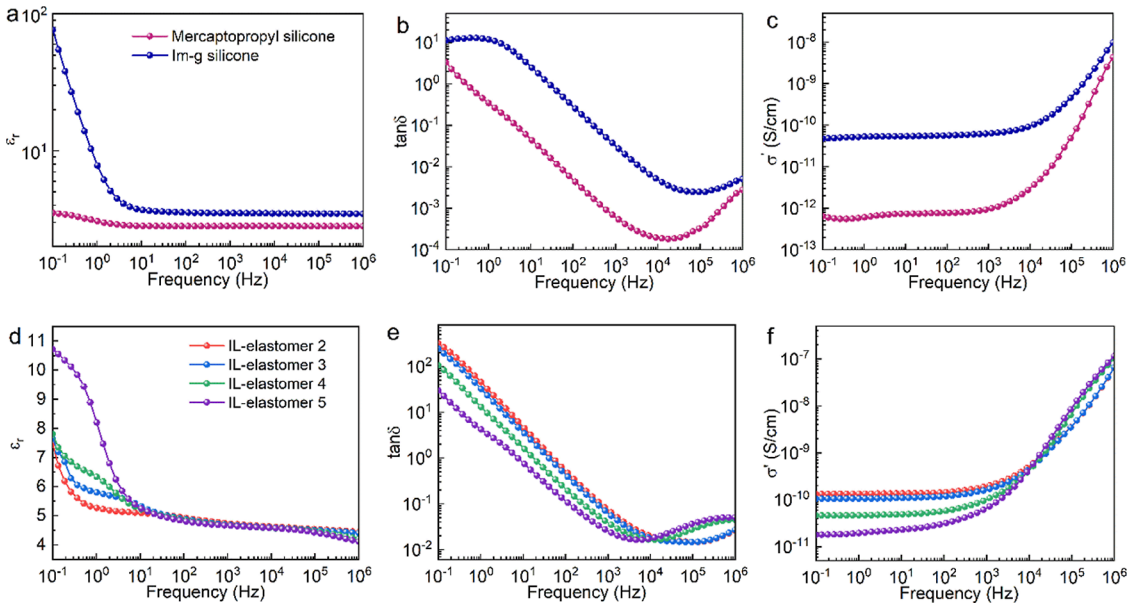

Figure 4. (a) Relative dielectric permittivity (ε_r), (b) loss tangent (tan δ), and (c) conductivity (σ') of the mercaptopropyl silicone and Im-g silicone, respectively, and (d) ε_r, (e) tan δ, and (f) σ' of IL-elastomers 2−5.

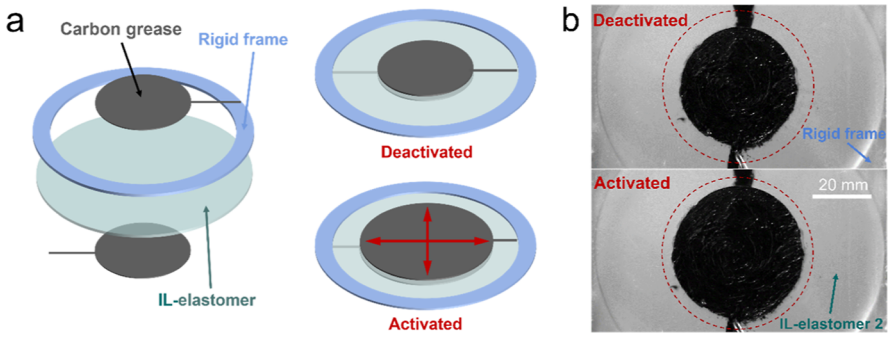

Figure 5. (a) Illustration of the preparation of the DEA and its deactivated and activated states and (b) images of the original and activated state (electric field 15 V/μm) of IL-elastomer 2.

contributes to increased actuation strain according to eq 1. The low Y can be attributed to the softening effect of the IL and unreacted moieties in the elastomer. Moreover, Y increases from 0.04 to 0.30 MPa with increasing $w''_{\text{bis-IL}}$ from 6.4 to 10.7 wt %. This can be attributed to the increased crosslinking density for the IL-elastomer with a high $w''_{\text{bis-IL}}$. Almost constant Y and strain at break were observed for all IL-elastomers stored in an ambient atmosphere for a year, again indicating the robustness of the crosslinking scheme hindering the aggregation of the highly stable IL[47] (Table S4).

The rheological properties are shown in Figure 3c. The storage modulus (G') increases with increased bis-IL content, which fits well the tensile results. In addition, the viscoelastic loss factors of all elastomers are below 0.1 at 10^{-2} Hz, indicating good mechanical integrity.[25,35] The mechanical stability of the IL-elastomers in cyclic strain was evaluated by uniaxial cyclic tensile experiments. Figure 3d shows cyclic stress−strain curves for IL-elastomers tested to 50% strain. All IL-elastomers present stable mechanical properties as evidenced by the good recoverability and negligible hysteresis. Stable mechanical properties are recorded for IL-elastomer 2 for more than 1000 cycles (Figure S5).

3.6. Dielectric Properties. The difunctional IL is solely utilized not only as the crosslinker to prepare mechanically stable elastomers but also to improve the relative permittivity of the elastomers due to its high polarity. The dielectric properties of the Im-g silicone and IL-elastomers are shown in Figure 4. Due to the grafted polar imidazole groups, the Im-g silicone shows a higher ε_r (76.4@0.1 Hz, 3.5@10^6 Hz) than that of the mercaptopropyl silicone (3.5@0.1 Hz, 2.8@10^6 Hz). As illustrated in Figure 4d and Table S5, all IL-elastomers have much higher relative permittivity than that of the mercaptopropyl silicone and those of a commonly used silicone elastomer, Sylgard 184, with $\varepsilon_r \sim 2.8$ measured at 0.1 Hz.[48] Furthermore, with increased bis-IL content, ε_r at 0.1 Hz increases from 7.5 for IL-elastomer 2 to 10.7 for IL-elastomer 5. The increase of ε_r is due to the intensified ionic polarization.[49,50] In addition, all IL-elastomers display a drastic decrease in ε_r with increasing frequencies from 0.1 to 10 Hz, and the ε_r decreases slowly with further increasing frequency to 10^6 Hz. This is consistent with the dielectric behavior of the Im-g silicone in Figure 4a, as the imidazole group and IL as dipoles cannot follow the rapid alternation of the electrical field above ~10 Hz.[51]

As shown in Figure 4b,c,e,f, compared with the mercaptopropyl silicone, the Im-g silicone and IL-elastomers exhibit higher loss tangent and conductivity due to the chemical modification with polar imidazole and IL, as expected.

https://doi.org/10.1021/acsami.2c16086
ACS Appl. Mater. Interfaces 2022, 14, 51384−51393

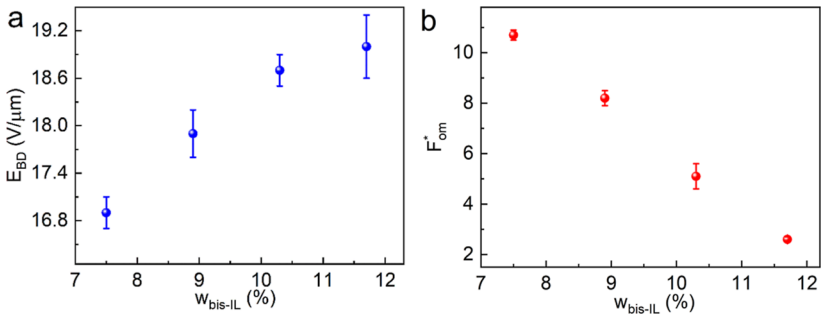

Figure 6. (a) Actual electric breakdown strength (E_{BD}) of IL-elastomers 2−5 determined from actuation tests and (b) normalized figure of merit (F^*_{om}) of IL-elastomers 2−5.

However, tan δ and σ' of the IL-elastomers decrease with increasing bis-IL content (from IL-elastomer 2 to IL elastomer 5) at frequencies of 10^{-1} to 10^4 Hz. This can be attributed to the decreased ion and chain mobilities in the elastomers with higher crosslinking densities, albeit the polar and ionic moieties are present in larger concentrations.

All investigated IL-elastomers are shown to be electrically insulating and potential candidates for actuator applications since their σ' at 0.1 Hz is below 10^{-9} S/cm.[11,15] Previously reported actuators based on dielectric elastomers exhibited high actuation strains, albeit they had high tan δ values but stability over time was not measured.[15] The investigated IL-elastomers present excellent dielectric stability over time due to negligible changes in ε_r, tan δ, and σ' after storage under ambient condition for a year (Figure S6). Thus, the properties of the novel IL-elastomers with outstanding ε_r (7.5−10.7@0.1 Hz) and Y (0.04−0.30 MPa) merit additional investigation as actuators.

3.7. Actuation Performance. Circular actuator devices were assembled by using the IL-elastomers and carbon grease as dielectric elastomer and electrodes, respectively. As illustrated in Figure 5a, the elastomer layer is sandwiched by electrodes, and combined Coulombic forces and Maxwell stress act to compress the thickness of the film and expand it in the plane when subjected to the electric field.[10] Figure 5b shows the IL-elastomer 2 before and after applying an electric field of 15 V/μm. An obvious expansion in area was observed in the activated state.

As shown in Figure 6a, the electrical breakdown strength E_{BD} of the IL-elastomers, recorded directly in the actuation tests, increased from 16.9 to 19.0 V/μm with increasing bis-IL content from 7.5 to 11.7 wt %. The increase of E_{BD} is due to the increased Y of the IL-elastomer with high content of the bis-IL crosslinker (Figure 3b).[24] In addition, the reduced σ' of IL-elastomers with increasing bis-IL content (Figure 4f) contributes to increased E_{BD}.[25]

A normalized figure of merit (F^*_{om}), which accounts for the respective parameters of the IL-elastomers as an actuator, was used to evaluate their theoretical actuation performance.[39] As shown in Figure 6b, all IL-elastomers have F^*_{om} values above 1, and thus, all investigated IL-elastomers present a better actuation performance than that of the reference elastomer, albeit their E_{BD} values are around half of that of the reference elastomer. In addition, the F^*_{om} decreases with increasing w_{bis-IL}. The highest F^*_{om} (10.7) was achieved by IL-elastomer 2 with the lowest bis-IL content (7.5%) among the IL-elastomers. IL-elastomers with a bis-IL content below 7.5% were not evaluated due to their low crosslinking densities, so they are not viable actuators. Summing up, the optimal actuation performance of the investigated IL-elastomers is governed by the lower limit for network structure integrity and the effect of increased dielectric permittivity plays a less significant role.

Figure 7a summarizes the results obtained in the actuation tests. All investigated IL-elastomers actuate with the increased

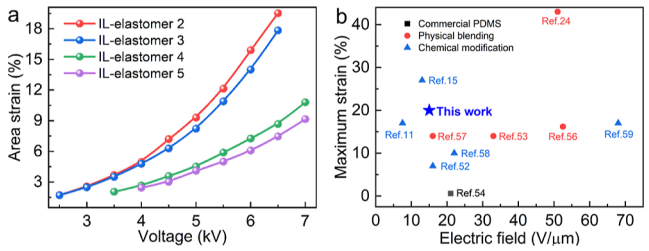

Figure 7. (a) Area strain of IL-elastomers 2−5 as a function of the voltage and (b) comparison of area actuation strains for differently modified silicone-based dielectric elastomers.

driving voltage before undergoing dielectric breakdown. A maximum area strain of 20% was achieved at 6.5 kV for IL-elastomer 2 with 7.5 wt % bis-IL. However, with increasing bis-IL content in the elastomer matrices, IL-elastomer 3 (8.9 wt % bis-IL) shows a maximum strain of 18% at 6.5 kV, and IL-elastomers 4 (10.3 wt % bis-IL) and 5 (11.7 wt % bis-IL) show maximum strains of 11 and 9% at 7 kV, respectively. This trend was also predicted from the normalized figures of merit (Figure 6b). The reduction of the actuation strain for the IL-elastomer with a high bis-IL content is attributed to the increased Y (Figure 3b), although the elastomer presents increased ε_r and E_{BD}. Therefore, IL-elastomer 2 shows the best actuation performance in both theory and experiment. Its actuation was recorded and is illustrated in Video S1 (Supporting Information). Furthermore, as shown in Figure S7, the area strain of the IL-elastomer 2 decreases from 14.5 to 8.5% at 5.5 kV with increased frequency of the electric field from 0.1 to 100 Hz. This is in agreement with the decreased relative permittivity with increasing frequency. Figure S8 shows the long-term actuation performance of the actuator based on IL-elastomer 2, where it is shown that the actuator endures 870 cyclic actuations under a continuously sinusoidal voltage of 6.0 kV at a frequency of 0.1 Hz.

An area strain comparison of IL-elastomer 2 and previously reported dielectric elastomers was performed. As shown in Figure 7b and Table S6, IL-elastomer 2 undergoes a higher area strain in a relatively low electric field (<30 V/μm) than the commercial elastomer Sylgard 184 and most filler-modified and chemically modified PDMS elastomers.[11,15,16,24,27,52−59] Interestingly, IL-elastomer 2 achieved the 3 times higher

https://doi.org/10.1021/acsami.2c16086
ACS Appl. Mater. Interfaces 2022, 14, 51384−51393

actuation strain than the PDMS elastomer modified with polyaniline in a similar electric field. The high actuation strain of the novel IL-elastomer highlights the potential of the proposed strategy to prepare a high-performance actuator with difunctional IL.

4. CONCLUSIONS

A novel approach to prepare PDMS elastomers via the crosslinking of synthesized multifunctional imidazole-grafted PDMS has been developed. The DEA with a bis-IL content of 7.5% presented a high area strain of 20% for an electrical field of as little as 15 V/μm. The actuation performance is achieved from a combination of excellent mechanical and dielectric properties of the IL-elastomer but mainly due to the excellent mechanical integrity of the elastomer at low crosslinking density. Due to the strategy of covalently incorporating of IL, the prepared IL-elastomer has a uniform dispersion of IL and presents stable mechanical and dielectric properties. The IL-elastomer presents an ϵ_r of 7.5, which is double that of the mercaptopropyl silicone. In terms of mechanical properties, this IL-elastomer has a relatively low Y (0.04 MPa) and high strain at break (182%). A normalized figure of merit of 10.7 compared to that of the reference pure PDMS elastomer was achieved despite the relatively low E_{BD} (~17 V/μm) of the elastomer. The exceptional actuation performance of this dielectric elastomer material suggests a promise for use in electroactive devices.

■ ASSOCIATED CONTENT

Supporting Information

The Supporting Information is available free of charge at https://pubs.acs.org/doi/10.1021/acsami.2c16086.

^{1}H NMR spectra of the eluted products of the IL-elastomers; gel fractions, weight fraction of bis-IL as the crosslinker, and the content of bis-IL as the crosslinker accounts for the whole bis-IL; crosslink density of the IL-elastomers; photographs of the IL-elastomers; FE-SEM images of the IL-elastomers; EDS images of IL-elastomer 3; TGA curves of the IL-elastomers; mechanical properties of the IL-elastomers after being stored under ambient condition for a year; cyclic stress−strain (1000) curves up to 50% strain for IL-elastomers 2; dielectric properties of the IL-elastomers at frequencies of 10^{-1} and 10^6 Hz; dielectric properties of IL-elastomers 2 and 4 after being stored a year under ambient condition; area strain as a function of frequency for IL-elastomer 2; cyclic actuation of IL-elastomer 2 under a sinusoidal voltage of 6000 V with a frequency of 0.1 Hz; and dielectric, mechanical, and actuation properties of previously reported PDMS dielectric actuators (PDF)

Actuation of IL-elastomer 2 (MP4)

■ AUTHOR INFORMATION

Corresponding Authors

Yi Nie − *CAS Key Laboratory of Green Process and Engineering, Beijing Key Laboratory of Ionic Liquids Clean Process, State Key Laboratory of Multiphase Complex Systems, Institute of Process Engineering, Chinese Academy of Sciences, Beijing 100190, China;* orcid.org/0000-0002-4111-6136; Email: ynie@ipe.ac.cn

Anne Ladegaard Skov − *Danish Polymer Center, Department of Chemical and Biochemical Engineering, Technical University of Denmark, Kgs. Lyngby 2800, Denmark;* orcid.org/0000-0003-1223-6638; Email: al@kt.dtu.dk

Authors

Zhaoqing Kang − *Danish Polymer Center, Department of Chemical and Biochemical Engineering, Technical University of Denmark, Kgs. Lyngby 2800, Denmark; CAS Key Laboratory of Green Process and Engineering, Beijing Key Laboratory of Ionic Liquids Clean Process, State Key Laboratory of Multiphase Complex Systems, Institute of Process Engineering, Chinese Academy of Sciences, Beijing 100190, China*

Liyun Yu − *Danish Polymer Center, Department of Chemical and Biochemical Engineering, Technical University of Denmark, Kgs. Lyngby 2800, Denmark*

Complete contact information is available at: https://pubs.acs.org/10.1021/acsami.2c16086

Notes

The authors declare no competing financial interest.

■ ACKNOWLEDGMENTS

This work was supported financially by the Department of Chemical and Biochemical Engineering, Technical University of Denmark, and the National Natural Science Foundation of China (grant no. 22178342).

■ REFERENCES

(1) Hartmann, F.; Baumgartner, M.; Kaltenbrunner, M. Becoming Sustainable, The New Frontier in Soft Robotics. *Adv. Mater.* **2021**, *33*, 2004413.

(2) Ren, Z.; Kim, S.; Ji, X.; Zhu, W.; Niroui, F.; Kong, J.; Chen, Y. A High-Lift Micro-Aerial-Robot Powered by Low-Voltage and Long-Endurance Dielectric Elastomer Actuators. *Adv. Mater.* **2022**, *34*, 2106757.

(3) Sparrman, B.; du Pasquier, C.; Thomsen, C.; Darbari, S.; Rustom, R.; Laucks, J.; Shea, K.; Tibbits, S. Printed Silicone Pneumatic Actuators for Soft Robotics. *Addit. Manuf.* **2021**, *40*, 101860.

(4) Wallin, T. J.; Simonsen, L. E.; Pan, W.; Wang, K.; Giannelis, E.; Shepherd, R. F.; Mengüç, Y. 3D Printable Tough Silicone Double Networks. *Nat. Commun.* **2020**, *11*, 4000.

(5) Hu, L.; Wan, Y.; Zhang, Q.; Serpe, M. J. Harnessing the Power of Stimuli-Responsive Polymers for Actuation. *Adv. Funct. Mater.* **2020**, *30*, 1903471.

(6) Hajiesmaili, E.; Clarke, D. R. Dielectric Elastomer Actuators. *J. Appl. Phys.* **2021**, *129*, 151102.

(7) Qi, D.; Zhang, K.; Tian, G.; Jiang, B.; Huang, Y. Stretchable Electronics Based on PDMS Substrates. *Adv. Mater.* **2021**, *33*, 2003155.

(8) Zhao, Q.; Chang, Y.; Yu, Z.; Liang, Y.; Ren, L.; Ren, L. Bionic Intelligent Soft Actuators: High-Strength Gradient Intelligent Hydrogels with Diverse Controllable Deformations and Movements. *J. Mater. Chem. B* **2020**, *8*, 9362−9373.

(9) Skov, A. L.; Yu, L. Optimization Techniques for Improving the Performance of Silicone-Based Dielectric Elastomers. *Adv. Eng. Mater.* **2018**, *20*, 1700762.

(10) Brochu, P.; Pei, Q. Advances in Dielectric Elastomers for Actuators and Artificial Muscles. *Macromol. Rapid Commun.* **2010**, *31*, 10−36.

(11) Perju, E.; Shova, S.; Opris, D. M. Electrically Driven Artificial Muscles Using Novel Polysiloxane Elastomers Modified with Nitroaniline Push-Pull Moieties. *ACS Appl. Mater. Interfaces* **2020**, *12*, 23432−23442.

(12) Madsen, F. B.; Daugaard, A. E.; Hvilsted, S.; Skov, A. L. The Current State of Silicone-Based Dielectric Elastomer Transducers. *Macromol. Rapid Commun.* **2016**, *37*, 378−413.
(13) Pelrine, R. E.; Kornbluh, R. D.; Joseph, J. P. Electrostriction of Polymer Dielectrics with Compliant Electrodes as a Means of Actuation. *Sens. Actuators, A* **1998**, *64*, 77−85.
(14) Poulin, A.; Rosset, S.; Shea, H. R. Printing Low-Voltage Dielectric Elastomer Actuators. *Appl. Phys. Lett.* **2015**, *107*, 244104.
(15) Sheima, Y.; Caspari, P.; Opris, D. M. Artificial Muscles: Dielectric Elastomers Responsive to Low Voltages. *Macromol. Rapid Commun.* **2019**, *40*, 1900205.
(16) Bele, A.; Dascalu, M.; Tugui, C.; Stiubianu, G. T.; Varganici, C. D.; Racles, C.; Cazacu, M.; Skov, A. L. Soft Silicone Elastomers Exhibiting Large Actuation Strains. *J. Appl. Polym. Sci.* **2022**, *139*, 52261.
(17) Hu, P.; Madsen, J.; Skov, A. L. One Reaction to Make Highly Stretchable or Extremely Soft Silicone Elastomers from Easily Available Materials. *Nat. Commun.* **2022**, *13*, 370.
(18) Hu, P.; Albuquerque, F. B.; Madsen, J.; Skov, A. L. Highly Stretchable Silicone Elastomer Applied in Soft Actuators. *Macromol. Rapid Commun.* **2022**, *43*, 2100732.
(19) Yu, L.; Skov, A. L. Silicone Rubbers for Dielectric Elastomers with Improved Dielectric and Mechanical Properties as a Result of Substituting Silica with Titanium Dioxide. *Int. J. Smart Nano Mater.* **2015**, *6*, 268−289.
(20) Yu, L.; Skov, A. L. ZnO as a Cheap and Effective Filler for High Breakdown Strength Elastomers. *RSC Adv.* **2017**, *7*, 45784−45791.
(21) Zhang, J.; Zhao, F.; Zuo, Y.; Zhang, Y.; Chen, X.; Li, B.; Zhang, N.; Niu, G.; Ren, W.; Ye, Z. Improving Actuation Strain and Breakdown Strength of Dielectric Elastomers Using Core-Shell Structured CNT-Al_2O_3. *Compos. Sci. Technol.* **2020**, *200*, 108393.
(22) Opris, D. M. Polar Elastomers as Novel Materials for Electromechanical Actuator Applications. *Adv. Mater.* **2018**, *30*, 1703678.
(23) Liu, J.; Yao, Y.; Li, X.; Zhang, Z. Fabrication of Advanced Polydimethylsiloxane-Based Functional Materials: Bulk Modifications and Surface Functionalizations. *Chem. Eng. J.* **2021**, *408*, 127262.
(24) Gale, C. B.; Brook, M. A.; Skov, A. L. Compatibilization of Porphyrins for Use as High Permittivity Fillers in Low Voltage Actuating Silicone Dielectric Elastomers. *RSC Adv.* **2020**, *10*, 18477−18486.
(25) Madsen, F. B.; Yu, L.; Daugaard, A. E.; Hvilsted, S.; Skov, A. L. Silicone Elastomers with High Dielectric Permittivity and High Dielectric Breakdown Strength Based on Dipolar Copolymers. *Polymer* **2014**, *55*, 6212−6219.
(26) Madsen, P. J.; Yu, L.; Boucher, S.; Skov, A. L. Enhancing the Electro-Mechanical Properties of Polydimethylsiloxane Elastomers through Blending with Poly (Dimethylsiloxane-co-Methylphenylsiloxane) Copolymers. *RSC Adv.* **2018**, *8*, 23077−23088.
(27) Kussmaul, B.; Risse, S.; Kofod, G.; Waché, R.; Wegener, M.; McCarthy, D. N.; Krüger, H.; Gerhard, R. Enhancement of Dielectric Permittivity and Electromechanical Response in Silicone Elastomers: Molecular Grafting of Organic Dipoles to the Macromolecular Network. *Adv. Funct. Mater.* **2011**, *21*, 4589−4594.
(28) Liu, M.; Yu, L.; Vudayagiri, S.; Skov, A. L. Incorporation of Liquid Fillers into Silicone Foams to Enhance the Electro-Mechanical Properties. *Int. J. Smart Nano Mater.* **2020**, *11*, 11−23.
(29) Liu, X.; Yu, L.; Zhu, Z.; Nie, Y.; Skov, A. L. Silicone-Ionic Liquid Elastomer Composite with Keratin as Reinforcing Agent Utilized as Pressure Sensor. *Macromol. Rapid Commun.* **2021**, *42*, 2000602.
(30) Style, R. W.; Boltyanskiy, R.; Allen, B.; Jensen, K. E.; Foote, H. P.; Wettlaufer, J. S.; Dufresne, E. R. Stiffening Solids with Liquid Inclusions. *Nat. Phys.* **2015**, *11*, 82−87.
(31) Style, R. W.; Tutika, R.; Kim, J. Y.; Bartlett, M. D. Solid-Liquid Composites for Soft Multifunctional Materials. *Adv. Funct. Mater.* **2021**, *31*, 2005804.
(32) Ankit; Tiwari, N.; Ho, F.; Krisnadi, F.; Kulkarni, M. R.; Nguyen, L. L.; Koh, S. J. A.; Mathews, N. High-K, Ultrastretchable Self-Enclosed Ionic Liquid-Elastomer Composites for Soft Robotics and Flexible Electronics. *ACS Appl. Mater. Interfaces* **2020**, *12*, 37561−37570.
(33) Shi, L.; Zhang, C.; Du, Y.; Zhu, H.; Zhang, Q.; Zhu, S. Improving Dielectric Constant of Polymers through Liquid Electrolyte Inclusion. *Adv. Funct. Mater.* **2021**, *31*, 2007863.
(34) Silau, H.; Stabell, N. B.; Petersen, F. R.; Pham, M.; Yu, L.; Skov, A. L. Weibull Analysis of Electrical Breakdown Strength as an Effective Means of Evaluating Elastomer Thin Film Quality. *Adv. Eng. Mater.* **2018**, *20*, 1800241.
(35) Liu, X.; Yu, L.; Nie, Y.; Skov, A. L. Silicone Elastomers with High-Permittivity Ionic Liquids Loading. *Adv. Eng. Mater.* **2019**, *21*, 1900481.
(36) Wasserscheid, P.; Keim, W. Ionic Liquids—New "Solutions" for Transition Metal Catalysis. *Angew. Chem., Int. Ed.* **2000**, *39*, 3772−3789.
(37) Kang, Z.; Yu, L.; Skov, A. L.A Novel PDMS Dielectric Elastomer Actuator with Bis-ionic liquid as Crosslinker. *Electroactive Polymer Actuators and Devices (EAPAD) XXIV*; International Society for Optics and Photonics, 2022; pp 335−341.
(38) Patel, S. K.; Malone, S.; Cohen, C.; Gillmor, J. R.; Colby, R. H. Elastic Modulus and Equilibrium Swelling of Poly (Dimethylsiloxane) Networks. *Macromolecules* **1992**, *25*, 5241−5251.
(39) Sommer-Larsen, P.; Larsen, A. L.Materials for Dielectric Elastomer Actuators, Smart Structures and Materials. *Electroactive Polymer Actuators and Devices (EAPAD)*; International Society for Optics and Photonics, 2004; pp 68−77.
(40) Yu, L.; Madsen, F. B.; Hvilsted, S.; Skov, A. L. Dielectric Elastomers, with very High Dielectric Permittivity, Based On Silicone and Ionic Interpenetrating Networks. *RSC Adv.* **2015**, *5*, 49739−49747.
(41) Yu, L.; Skov, A. L. Molecular Strategies for Improved Dielectric Elastomer Electrical Breakdown Strengths. *Macromol. Rapid Commun.* **2018**, *39*, 1800383.
(42) Müller, A.; Wapler, M. C.; Wallrabe, U. A Quick and Accurate Method to Determine the Poisson's Ratio and the Coefficient of Thermal Expansion of PDMS. *Soft Matter* **2019**, *15*, 779−784.
(43) Jheng, L.; Hsu, S. L. C.; Lin, B.; Hsu, Y. Quaternized Polybenzimidazoles with Imidazolium Cation Moieties for Anion Exchange Membrane Fuel Cells. *J. Membr. Sci.* **2014**, *460*, 160−170.
(44) Kadari, M.; Belarbi, E. H.; Moumene, T.; Bresson, S.; Haddad, B.; Abbas, O.; Khelifa, B. Comparative Study between 1-Propyl-3-Methylimidazolium Bromide and Trimethylene Bis-Methylimidazolium Bromide Ionic Liquids By FTIR/ATR and FT-RAMAN Spectroscopies. *J. Mol. Struct.* **2017**, *1143*, 91−99.
(45) Kang, Z.; Nie, Y.; Yu, L.; Zhang, S.; Skov, A. L. Highly Sensitive Flexible Pressure Sensors Enabled by Mixing of Silicone Elastomer with Ionic Liquid-Grafted Silicone Oil. *Front. Robot. AI* **2021**, *8*, 737500.
(46) Li, F.; Larock, R. C. New Soybean Oil-Styrene-Divinylbenzene Thermosetting Copolymers. III. Tensile Stress−Strain Behavior. *J. Polym. Sci., Part B: Polym. Phys.* **2001**, *39*, 60−77.
(47) Smiglak, M.; Pringle, J. M.; Lu, X.; Han, L.; Zhang, S.; Gao, H.; MacFarlane, D. R.; Rogers, R. D. Ionic Liquids for Energy, Materials, and Medicine. *Chem. Commun.* **2014**, *50*, 9228−9250.
(48) Vaicekauskaite, J.; Mazurek, P.; Vudayagiri, S.; Skov, A. L. Mapping the Mechanical and Electrical Properties of Commercial Silicone Elastomer Formulations for Stretchable Transducers. *J. Mater. Chem. C* **2020**, *8*, 1273−1279.
(49) El-Haddad, M. N.; Fouda, A. S. Electroanalytical Quantum and Surface Characterization Studies on Imidazole Derivatives as Corrosion Inhibitors for Aluminum In Acidic Media. *J. Mol. Liq.* **2015**, *209*, 480−486.
(50) Pinilla, C.; Del Pópolo, M. G.; Kohanoff, J.; Lynden-Bell, R. M. Polarization Relaxation in an Ionic Liquid Confined between Electrified Walls. *J. Phys. Chem. B* **2007**, *111*, 4877−4884.
(51) Weingärtner, H.; Sasisanker, P.; Daguenet, C.; Dyson, P. J.; Krossing, I.; Slattery, J. M.; Schubert, T. The Dielectric Response of

Room-Temperature Ionic Liquids: Effect of Cation Variation. *J. Phys. Chem. B* **2007**, *111*, 4775−4780.
(52) Duan, L.; Lai, J.; Li, C.; Zuo, J. A Dielectric Elastomer Actuator That Can Self-Heal Integrally. *ACS Appl. Mater. Interfaces* **2020**, *12*, 44137−44146.
(53) Liu, L.; Lei, Y.; Zhang, Z.; Liu, J.; Lv, S.; Guo, Z. Fabrication Of PDA@SiO_2@rGO/PDMS Dielectric Elastomer Composites with Good Electromechanical Properties. *React. Funct. Polym.* **2020**, *154*, 104656.
(54) Risse, S.; Kussmaul, B.; Krüger, H.; Kofod, G. A Versatile Method for Enhancement of Electromechanical Sensitivity of Silicone Elastomers. *RSC Adv.* **2012**, *2*, 9029−9035.
(55) Albuquerque, F. B.; Shea, H. Influence of Humidity, Temperature and Prestretch on the Dielectric Breakdown Strength of Silicone Elastomer Membranes for DEAs. *Smart Mater. Struct.* **2020**, *29*, 105024.
(56) Yang, T.; Liu, L.; Li, X.; Zhang, L. High Performance Silicate/Silicone Elastomer Dielectric Composites. *Polymer* **2022**, *240*, 124470.
(57) Dascalu, M.; Iacob, M.; Tugui, C.; Bele, A.; Stiubianu, G. T.; Racles, C.; Cazacu, M. Octakis (Phenyl)-T8-Silsesquioxane-Filled Silicone Elastomers with Enhanced Electromechanical Capability. *J. Appl. Polym. Sci.* **2021**, *138*, 50161.
(58) Liu, X.; Sun, H.; Liu, S.; Jiang, Y.; Yu, B.; Ning, N.; Tian, M.; Zhang, L. Mechanical, Dielectric and Actuated Properties of Carboxyl Grafted Silicone Elastomer Composites Containing Epoxy-Functionalized TiO_2 Filler. *Chem. Eng. J.* **2020**, *393*, 124791.
(59) Zhang, L.; Wang, D.; Hu, P.; Zha, J.; You, F.; Li, S.; Dang, Z. Highly Improved Electro-Actuation of Dielectric Elastomers by Molecular Grafting of Azobenzenes to Silicon Rubber. *J. Mater. Chem. C* **2015**, *3*, 4883−4889.

https://doi.org/10.1021/acsami.2c16086
ACS Appl. Mater. Interfaces 2022, 14, 51384−51393